

Nonlinear Dynamic Analysis of Concrete Arch Dams

Javad Moradloo¹, Mohammad Taghi Ahmadi², Shahram Vahdani³

¹ Assistant Professor, School of Engineering, University of Zanjan, Zanjan, Iran

² Professor of Civil Engineering, School of Engineering, Tarbiat Modarres University, Tehran, Iran

³ Assistant Professor, School of Engineering, University of Tehran, Tehran, Iran

Email: mahmadi@modares.ac.ir, ajmoradloo@yahoo.com, shvahdani@ut.ac.ir

ABSTRACT :

In this study, nonlinear dynamic analysis of concrete arch dam is presented. A three dimensional smeared crack model is used to consider nonlinear behavior of mass concrete. The proposed model considers major characteristics of mass concrete under three dimensional loading conditions. These characteristics are pre-softening behavior, softening initiation criteria, fracture energy conservation and strain rate effect. After verification of the proposed model by some available numerical tests, dynamic analysis of the Morrow Point concrete arch dam under the three components of the Taft earthquake scaled to 1.0g is carried out. In the present analysis, complete fluid-structure interaction is considered accounting for fluid compressibility and absorptive reservoir boundary condition appropriately. The coupled equation resulting from dam-reservoir interaction was solved using staggered method. The deduced results show that crack pattern has good agreement with the contour of maximum principal stresses. The proposed algorithm also gives reliable solution even in large time steps.

KEYWORDS:

Arch Concrete Dam, Dynamic Analysis, Nonlinear, Smeared Crack, Fluid Structure Interaction

1. INTRODUCTION

Materially nonlinear behavior of concrete arch dam is the matter which can be arises under extreme loading. However two dimensional modeling, especially by smeared crack models has received more attention and it progressed considerably in the last decades. Three dimensional nonlinear modeling of concrete dam, however, received less attention and it needs more research to capture the arch dam real behavior under sever loading such as the MCL earthquake [1,2] .

Pekao et al.[3] used a model based on linear elastic fracture mechanics theory to simulate the nonlinear behavior of gravity dams. The boundary element method was used to discrization of dam and reservoir domain. Feng [4] investigated cracking of gravity dam using linear elastic fracture mechanics and boundary element method. The Kolnbrein arch dam was considered as the case study. Al-Eidi's research [5, 6] probably is the first study that used nonlinear fracture mechanics to simulate concrete dam behavior. Gunglun et al. [7] proposed a smeared crack model based on bezant's crack band theory. Bhattachjee and Leger [8] used a smeared crack model to conduct a seismic analyze of concrete gravity dam. Ghrib and Tinawi [9] proposed a new model based on continuum damage mechanics for seismic fracture analysis of gravity dam. Only one damage variable was considered for tensional damage. Faria [10] proposed a 3 dimensional damage mechanics model for analysis of gravity and arch concrete dam. Concrete was modeled by a isotopic model that capable for tensional and compression damage. Mizabozorg [11] used a three dimensional damage mechanics model to investigate nonlinear behavior of concrete arch dam. ACI [2] suggested that three dimensional crack modeling is in its initial stage of progress and every smeared and discrete crack models need to further investigation to apply in order to be adequately applicable to concrete structures.

In the present study the nonlinear dynamic analysis of concrete arch dam using rotating smeared crack model is presented. The proposed smeared crack model is capable of modeling of mass concrete damage in three-dimensional space. It simulates the tensile fracture on the mass concrete and contains pre-softening behavior, softening initiation, fracture energy conservation and strain rate effects under dynamic loads. Fluid-Structure dynamic interaction is fully considered by accurate finite element modeling of the Helmholtz equation. The solution method is a modified staggered method. Soil-Structure interaction is not considered here.

In the upcoming sections of this paper, the basic concepts and employed models are explained briefly at first. After model verification, the nonlinear dynamic behavior of Morrow Point arch dam is studied by the application of the models discussed.

2. BASIC CONSEPTS AND METHODOLOGY

2.1 Proposed Crack Model

A comprehensive numerical model in fracture mechanics analysis of mass concrete is should be able to simulate the behavior of concrete in different three stage conditions: Pre-softening behavior, Softening behavior and Crack closing/reopening behavior.

Based on older investigation a reliable smeared crack model must be having some minor but important components such as: softening initiation criteria, fracture energy conservation, damping mechanism for cracked element, characteristic Length and dynamic magnification factors for concrete parameters.

2.2.1 Pre-softening behavior modeling

In this study linear elastic behavior is considered as for the pre-softening stage of mass concrete.

2.2.2 Softening initiation Criterion

The uni-axial strain energy has been used as the softening initiation criterion. This criterion considers effects of other component of stress and strain and was used successfully in static and dynamic analysis of concrete dam [11,12]. Based on this criterion, the crack initiates when the uni-axial strain energy density is greater than material parameter:

$$U > U_0 \quad (2.1)$$

Where U is uni-axial strain energy density and equal with:

$$U = \frac{1}{2} s_1 e_1 \quad (2.2)$$

s_1, e_1 are the first principal stress and strain of an integration point respectively . U_0 is material parameter and equal with:

$$U_0 = \frac{1}{2} s_0 e_0 \quad (2.3)$$

Where s_0, e_0 are the apparent tensile strength and its corresponding strain respectively. Since the pre-peak stress-strain relationship is assumed to be linear, the apparent tensile strength is calibrated in such a way that a linear elastic uni-axial stress-strain relationship up to s_0 will preserve the value of U_0 . The above relations are valid for static loading conditions. Under dynamic loading material parameter is multiplied by a dynamic magnification factor DMF_t .

2.2.3 Softening behavior

After Crack initiation, the isotropic constitutive matrix is replaced with an orthotropic constitutive matrix, which their components are determined corresponds to the stiffness degradation level in the three principal direction stresses. In present study, the SMS (Secant Module Stiffness) approach has been employed for the stiffness formulation in which the constitutive relation is defined in terms of total stress and strain. Based on SMS formulation, the total strains on crack plane $\{\Delta e\}$ are decomposed into elastic $\{\Delta e^{co}\}$ and cracking $\{\Delta e^{cr}\}$ components:

$$\{\Delta e\} = \{\Delta e^{co}\} + \{\Delta e^{cr}\} \quad (2.4)$$

The superscript 'co' corresponds to the elastic components of total strain and superscript 'cr' correspond to cracked portion of total strain. The cracked strain is related to the corresponding cracked stress using the cracked constitutive matrix $[D^{cr}]$ as follows:

$$\{s^{cr}\} = [D^{cr}]^T \{e^{cr}\} \quad (2.5)$$

After some algebraic operations cracked constitutive matrix $[D]_s$ in the global coordinates system is given as [11,13]:

$$[D]_s = \left[[D^{co}] - [D^{co}] [T] [D^{cr}] + [T]^T [D^{co}] [T] \right]^{-1} [T]^T [D^{co}] \quad (2.6)$$

Where $[D^{co}]$ is the intact module matrix, $[T]$ is the transformation matrix which transforms the vector of cracked strain to the global coordinate direction. This matrix in rotating crack model is changed in every iteration, but at fixed crack model is constant after first crack initiation. In a special case, when crack plane normal is parallel to the global x direction and the two other tangential local directions are parallel to the other global directions, the total secant matrix in local co-ordinates is given as[11]:

$$[D]_{nst} = \begin{bmatrix} D_{11} & D_{12} & D_{13} & 0 & 0 & 0 \\ D_{21} & D_{22} & D_{23} & 0 & 0 & 0 \\ D_{31} & D_{32} & D_{33} & 0 & 0 & 0 \\ 0 & 0 & 0 & D_{44} & 0 & 0 \\ 0 & 0 & 0 & 0 & D_{55} & 0 \\ 0 & 0 & 0 & 0 & 0 & D_{66} \end{bmatrix} \quad (2.7)$$

Where:

$$\begin{aligned} D_{11} &= \frac{h_1 E (1 - n^2 h_2 h_3)}{1 - n^2 h_1 h_2 - n^2 h_3 h_2 - n^2 h_1 h_3 - 2n^3 h_1 h_2 h_3} & D_{22} &= \frac{h_2 E (1 - n^2 h_1 h_3)}{1 - n^2 h_1 h_2 - n^2 h_3 h_2 - n^2 h_1 h_3 - 2n^3 h_1 h_2 h_3} \\ D_{33} &= \frac{h_3 E (1 - n^2 h_2 h_1)}{1 - n^2 h_1 h_2 - n^2 h_3 h_2 - n^2 h_1 h_3 - 2n^3 h_1 h_2 h_3} & D_{12} &= \frac{nh_1 h_2 E (1 + nh_3)}{1 - n^2 h_1 h_2 - n^2 h_3 h_2 - n^2 h_1 h_3 - 2n^3 h_1 h_2 h_3} \\ D_{23} &= \frac{nh_3 h_2 E (1 + nh_1)}{1 - n^2 h_1 h_2 - n^2 h_3 h_2 - n^2 h_1 h_3 - 2n^3 h_1 h_2 h_3} & D_{13} &= \frac{nh_1 h_3 E (1 + nh_2)}{1 - n^2 h_1 h_2 - n^2 h_3 h_2 - n^2 h_1 h_3 - 2n^3 h_1 h_2 h_3} \\ D_{44} &= b_{12} G & D_{55} &= b_{23} G & D_{66} &= b_{13} G \quad , \\ h_i &= \frac{E_i^s}{E} \end{aligned} \quad (2.8)$$

The constitutive matrix in global coordinate system can be obtained as follows:

$$[D]_s = [T]^T [D]_{nst} [T] \quad (2.9)$$

Matrix $[T]$ is introduced earlier. Based on the maximum strain reached in each principal direction, the secant module matrix is determined as shown in Figure 2. Increasing the normal strain in each direction lead to reduction of corresponding softened young's modules. Finally, when the maximum strain reaches the fracture strain, integration

point in the corresponding direction is fully cracked and the softened young modules set to be zero.

In above equations b_{ij} are shear retention factors. In the earliest three-dimensional smeared crack models it was assumed that the softened shear moduli in two tangential directions were zero. In some situations it can lead to numerical problems. Some of the investigators assumed various empirical descending relations for shear module versus normal strain. In the proposed formulation based on concept of co-axially of fracture plane and principal stress, shear retention factors can be calculated easily:

$$G_s = \frac{S_1 - S_2}{2(e_1 - e_2)} \quad (2.10)$$

Where G_s is the softened shear modulus corresponding to i-j axes on the fracture plane and S_i , e_i are principal stresses and strains corresponding to the principal directions of j and j. Using equations (2.10), (2.4) the stress-strain relationship in three-dimensional space is given as :

$$e_n = \frac{1}{Eh_1}(s_n - nh_1s_s - nh_1s_t) \quad , \quad e_s = \frac{1}{Eh_2}(s_s - nh_2s_n - nh_2s_t) \quad , \quad e_t = \frac{1}{Eh_3}(s_t - nh_3s_n - nh_3s_s) \quad (2.11)$$

Combining Equations (2.10) and (2.11), the shear retention factors in equation (2.7) are determined as follows[11]:

$$\begin{aligned} b_{12} &= \frac{1+u}{1-u^2h_1h_2 - u^2h_3h_2 - u^2h_1h_3 - 2u^3h_1h_2h_3} \left(\frac{h_1e_1 - h_2e_2}{e_1 - e_2} + \frac{uh_3(h_1 - h_2)e_3}{e_1 - e_2} - uh_1h_2 - 2u^2h_1h_2h_3 \right) \\ b_{23} &= \frac{1+u}{1-u^2h_1h_2 - u^2h_3h_2 - u^2h_1h_3 - 2u^3h_1h_2h_3} \left(\frac{h_2e_2 - h_3e_3}{e_2 - e_3} + \frac{uh_1(h_2 - h_3)e_1}{e_2 - e_3} - uh_3h_2 - 2u^2h_1h_2h_3 \right) \\ b_{13} &= \frac{1+u}{1-u^2h_1h_2 - u^2h_3h_2 - u^2h_1h_3 - 2u^3h_1h_2h_3} \left(\frac{h_1e_1 - h_3e_3}{e_1 - e_2} + \frac{uh_2(h_1 - h_3)e_2}{e_1 - e_2} - uh_1h_3 - 2u^2h_1h_2h_3 \right) \end{aligned} \quad (2.12)$$

2.2.4 Crack closing/reopening behavior

Various models proposed to modeling loading/unloading in smeared crack approach [13]. In the present study the closing/reopening criterion is based on value of the principal strains. It has been shown that under cyclic loads there is residual strain in the closed crack. Based on this concept, the total strain can be decomposed into two components of recoverable elastic and residual strain given as[11]:

$$e = e^e + e^{res} = e^e + I e_{max} \quad (2.13)$$

Where e_{max} is the maximum principal strain which the point has experienced during the previous loading and I is the ratio between residual strain in the closed crack and the maximum principal strain and is given as 0.2 usually [11].

2.2.5 Damping mechanism for cracked element

It has been shown that conventional Rayleigh damping model could lead to numerical problems in seismic crack analysis. It seems mainly from mass proportional component of damping .In the present study the Elasto -Brittle Damping (EDM) and Linear Damping model (LDM) employed. In EDM model damping of cracked point equal zero, and in (LDM) model damping of cracked point is proportional with current stiffness of material.

2.2.6 Characteristic Length

In the present study it is assumed that the mesh size property which should be measured by the characteristic length, is equal to the cubic root of volume affected by integration point as:

$$h_c = \sqrt[3]{w_i w_j w_k \det J} \quad (2.14)$$

2.2.7 Fracture energy conservation

Fracture energy conservation is preserved once the following fracture strain is used:

$$e_f = \frac{2G_f}{h_c f_t} \quad (2.15)$$

Where : e_f , G_f , h_c , f_t are ultimate uni-axial strain , fracture energy , characteristic length and uni-axial tensile strength respectively. In dynamic loading, material parameters are magnified by related dynamic magnification factors.

2.2.8 Dynamic magnification factors for concrete parameters

It is shown that material parameters of concrete in dynamic loading are different from static values. It is mainly originate from fact that in dynamic loading crack passes across aggregate and since its strength, module of elasticity, fracture toughness will increases. A few studies were carried out based on viscoelastic models to consider strain rate effects on concrete behavior [11]. In the present study strain rate effects are modeled by proper dynamic magnification factors. In this way dynamic material parameters are given as:

$$G'_f = DMF_g G_f, \quad f'_t = DMF_t f_t, \quad E' = DMF_e E \quad (2.16)$$

Where primed parameters are related to dynamic values.

2.2.9 Proposed Crack Algorithm

In the present paper a Rotating Smeared crack model based on above relations is presented. Crack is considered in integration points. In Figure (1) calculation of stiffness matrix and internal forces is presented. Crack state determination flowchart is presented in Figure (2).

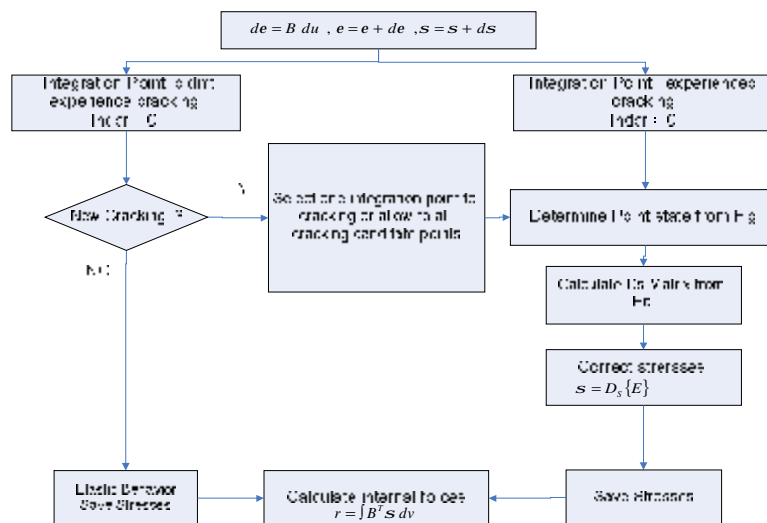


Figure 1 Stress , stiffness matrix and internal forces calculation algorithm [13]

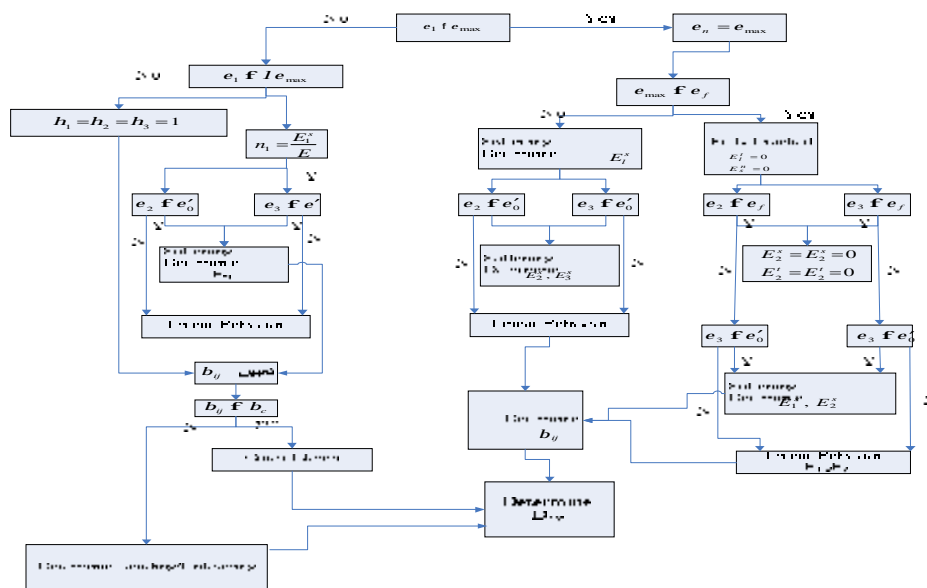


Figure 2 Algorithm for state determination of integration point

2.3 Fluid-Structure Interaction

The governing equation for fluid domain is the Helmholtz equation for hydrodynamic pressure:

$$\nabla^2 P = -\frac{1}{C^2} \ddot{p} \quad (2.17)$$

Where P, C are the hydrodynamic pressure and the acoustic wave velocity in water respectively. The above equation implies small displacements of inviscid compressible fluid with irrotational motion. Water compressibility has a significant influence on the fluid-structure interaction for a wide range of ratio of natural frequencies of structure to fluid domain, including the case of higher and stiffer dams [13]. Thus, for general applicability and completeness of the dam-reservoir formulation, one needs to include the reservoir water compressibility.

Boundary conditions for Helmholtz equation in a concrete dam – reservoir interaction problem are expressed as:

$$\left[\frac{\partial P}{\partial y} + \frac{1}{g} \ddot{p} \right]_{y=h} = 0 \quad (2.18)$$

That is called Cauchy Boundary Condition for the reservoir-free surface,

$$\frac{\partial P}{\partial n} = -r \ddot{a}_{ns} - \frac{1}{bC} \frac{\partial P}{\partial t} \quad (2.19)$$

For the reservoir bottom partial absorption and normal component of earthquake records

$$\frac{\partial P}{\partial x} = -\frac{p}{2h} P - \frac{1}{C} \frac{\partial P}{\partial t} \quad (2.20)$$

For the reservoir upstream face radiation of acoustic waves, and

$$r \ddot{a}_{ns} = -\frac{\partial P}{\partial n} \quad (2.21)$$

For the interaction boundary between dam and reservoir

In the above equations, z is the vertical coordinate, b, the acoustic impedance ratio of rock to water, n, the vector perpendicular to the boundary, r, the mass density of water, g, the gravitational acceleration, and \ddot{a}_{ns} , the absolute acceleration of dam upstream face in the normal direction. Here, we have assumed that the hydrodynamic waves satisfy the 1-D wave propagation equation (2.20), through the upstream reservoir near-field truncation surface. If we ignore first term at right hand of equation (2.20) this boundary, sometimes known as the Sommerfeld or viscous boundary, performs well in time domain analysis when applied sufficiently far from the structure. The above equations along with the governing equation for the structure would lead to a simultaneous differential equations set for the coupled dam –reservoir System. These equations are discretized by the finite element method in a standard way similar to that of Ref. [13]. To avoid prohibitively high number of nonsymmetrical equations with large bandwidth, the modified staggering solution method [13] is employed. Here, the displacement and the pressure fields are solved alternatively in each time step to achieve "inter-domain compatibility" or convergence.

2.4 Nonlinear Dynamic Analysis

In the present study, the Newmark standard scheme is used to integration of differential equation in time domain and the Newton –Raphson method is used to solve nonlinear equations.

3. COMPUTER IMPLEMENTATION AND VERIFICATION EXAMPLES

3.1 Computer Implementation

The proposed models have been implemented at finite element code GFEAP (Generalized Finite Element Code Program). GFEAP has capabilities of time history nonlinear dynamic analysis of arch dam, considering material, geometrical and construction joint nonlinearity and fluid structure interaction. It was prepared at Tarbiat Modares University (TMU) by writers for complete nonlinear dynamic analysis of gravity and arch concrete dams.

3.2 Preliminary example

The validity of the proposed models and numerical algorithms has been checked using the available numerical results [13]. Only one test is presented here. This model is a tension beam in which the ultimate load resistance has been

checked under direct displacement control approach in order to verify proposed smeared crack model. The three-dimensional tension beam with unit thickness under tension prescribed displacement (Fig3) is tested [13]. The used material parameters values module of elasticity, poisson ratio, tensile strength and the specific fracture energy have been assumed as 20 GPa, 0, 2.0 MPa and 40 N/m respectively. Strength of two elements near to supports is reduced for 5 % to concentrate the fracture at these elements.

The displacement and strain distribution are presented at Fig 4, Fig 5 respectively. As shown at this figures localization of fracture is evidence at weakened elements. The Displacement-Load curve is presented at Fig 6. As shown at these figures the ultimate load is 95 KN which is equal with analytical solution. The stress-strain curve of softened integration point is presented as fig 7. As shown at this figure, ultimate stress, crack initiation, fracture energy conservation and softening behavior are modeled properly.

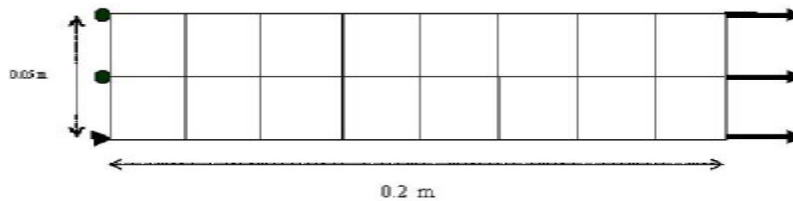


Figure 3 Geometry and finite element mesh of tension beam test

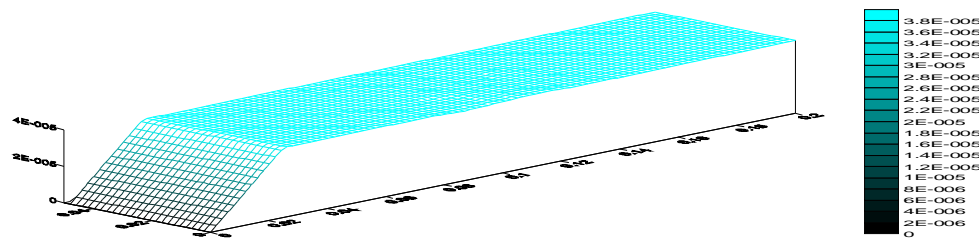


Figure 4 Displacement Distribution for prescribed displacement equal 0.00004 m

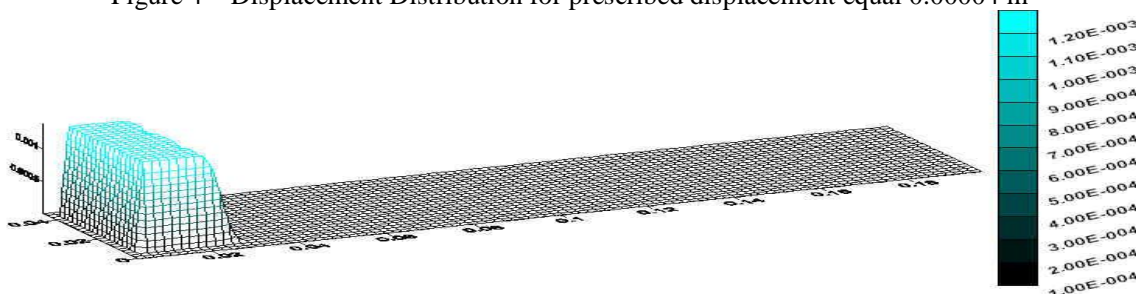


Figure 5 Strain Distribution for prescribed displacement equal 0.00004 m

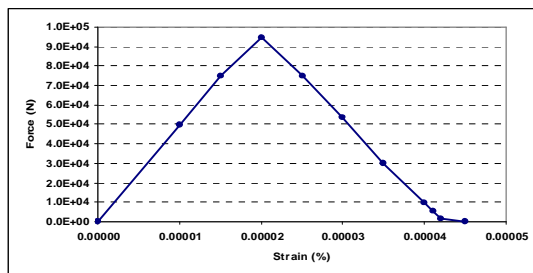


Figure 6 Load – Displacement curve

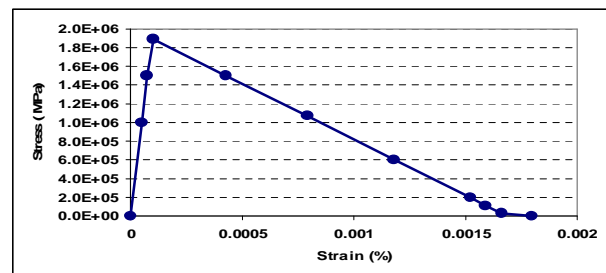


Figure 7 the stress – strain curve of softened element

4. APPLICATION ON CONCRETE ARCH DAMS

In this section, the nonlinear behavior of Morrow Point arch dam is being studied by application of the models

discussed above. The dam is 145 m high; with the width of valley at crown elevation is 184 m on the Gunnison River in Colorado, USA. This dam is approximately symmetric, single cantered arch dam. Detailed description of the geometry of this dam is available in Ref. [13]. Figure 8 shows the considered system which includes the finite element model of dam body and the reservoir in which the length of reservoir in the upstream direction is about nearly two times the height of dam. Moreover, the dam-foundation interaction is neglected. Sixteen 20-node solid element and 180 20-node fluid elements are used to modeling of dam body and reservoir domain respectively.

The modulus of elasticity, poisson ratio, density, tensile strength, fracture energy, dynamic magnification factors applied to tensile strength, modulus of elasticity, and fracture energy are 27GP, 0.2, 2483 kg/m³, 3MPa , 260Nm/m, 1.5, 1.25, and 1.8 respectively

Considered internal viscous damping ratio is 0.05 for first and fifth vibration modes. Water level elevation for both hydrostatic and hydrodynamic pressure calculations is equal to the dam crest elevation (141.73 m). Acoustic wave velocity in water is C, 1440.0 m/s. The acoustic impedance ratio of rock to water is, $b = 3.444$.

The ground motion recorded at Taft Lincoln School during the Kern County, California earthquake of 21 July 1952 is selected as the free-Field ground acceleration (Fig. 9). The records are scaled to 1 g .

The loads applied on the system are self weight, hydrostatic pressure and seismic load. The standard Newmark method is used to integration of dynamic equation in time domain. The Newmark parameters of a , b were assumed as 0.5, 0.25 respectively. The time integration steps were 0.01 and 0.005 alternatively. The elasto -Brittle Damping (EDM) and Linear Damping model (LDM) have been used in dynamic analysis. The 14 point integration rule is used in elements volume numerical integration. It was found that this integration scheme compared to costume 3*3*3 integration rule is economical. The analysis cases are presented in Table 1.

Table 1 Considered Analytical cases

<i>Case</i>	<i>Description</i>	<i>PGA</i>
A	EDM Damping model , Dt=0.01	1g
B	LDM Damping model, Dt=0.01	1g
C	EDM Damping model, Dt=0.005	1g

Figure 11 shows the time history of the crest displacement in the stream direction. The model did not experience any crack due to static loads. In the dynamic loading, the first crack appeared at the base level. The space distribution of cracked element, the time of cracking and the number of cracked integration points have been shown in Figs. 11,12 .The time history of the first principal stress at some cracked integration points are shown in figures 13,14. As shown the model is capable in softening modeling properly .In spite of the cracking of more than % 40 of the elements, the analysis is stable up to the end of the earthquake without any numerical instability. In cases A, and B only one integration point is permitted to crack in each iteration. Therefore deduced crack pattern in figs. 11,12is unsymmetrical.

Case C is repeated with a different time step of 0.005. Figure 16 shows the displacement time history of the dam crown with the two Dt values. Peak displacement is increased due to the reduced time step. Also as shown in Fig 17 the damage distribution has been also changed.

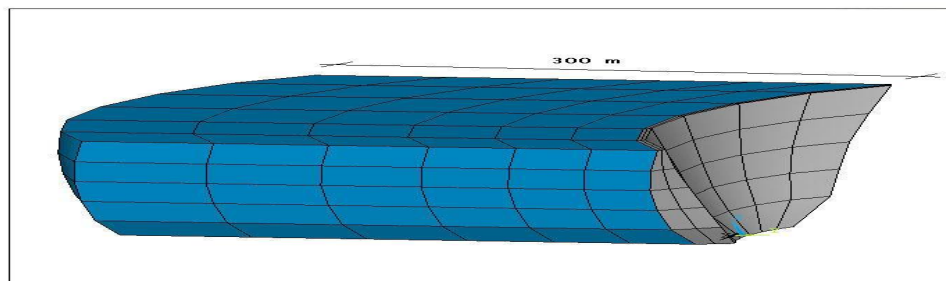
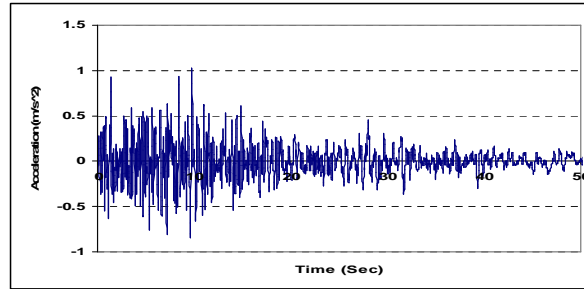
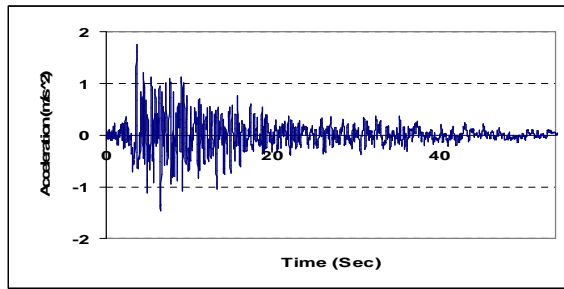
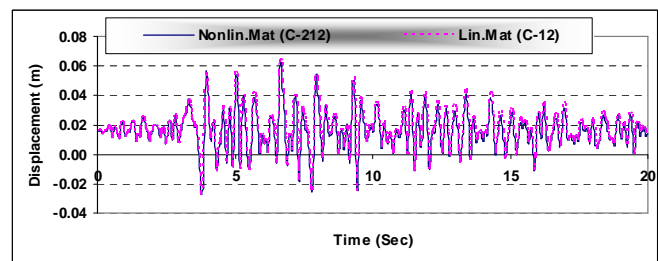
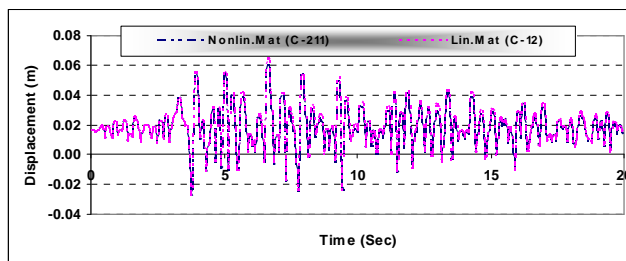


Figure 8 Dam-reservoir finite element model of Morrow Point arch dam.



Horizontal Component Vertical Component
 Figure 9 Original ground motion of Taft Lincoln California Earthquake of 21 July 1952.



Case A Case B
 Figure 10 Time history of crest displacement in stream direction

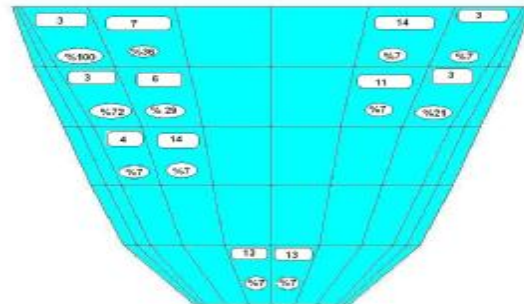
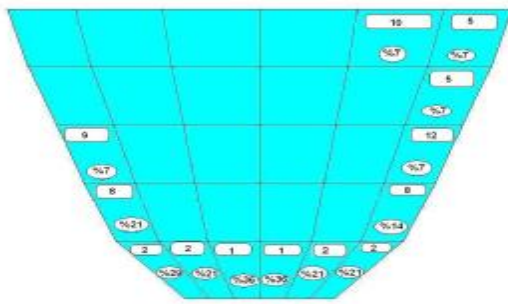


Figure 11 Distribution of damage in dam, Upstream and Downstream (Case A)

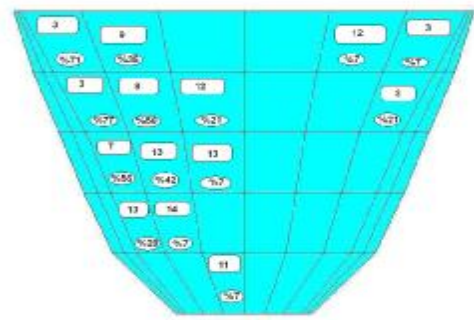
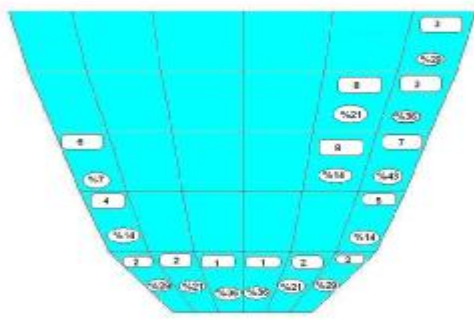


Figure 12 Distribution of damage in dam, Upstream and Downstream (Case B)

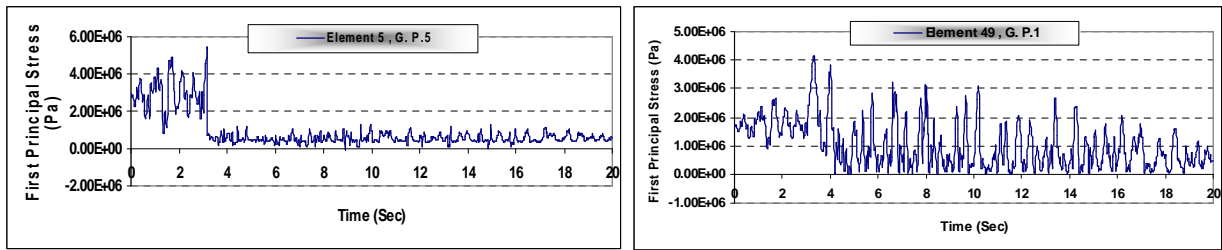


Figure 13 Time history of first principal stress in cracked integration point (First cracking time: 3.2 s) (Case A)

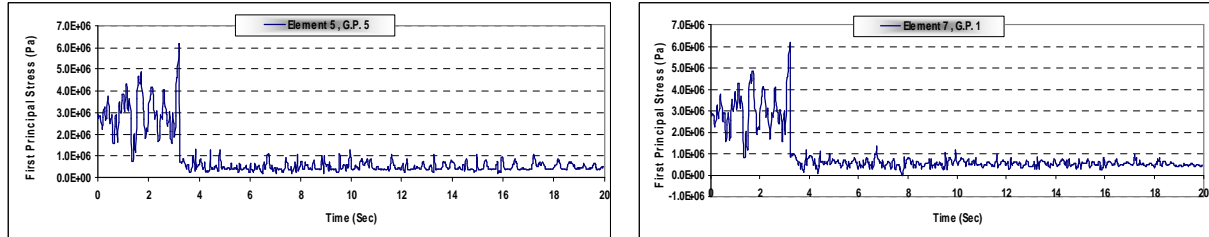


Figure 14 Time history of first principal stress in cracked integration point (First cracking time: 3.2 s) (Case B)

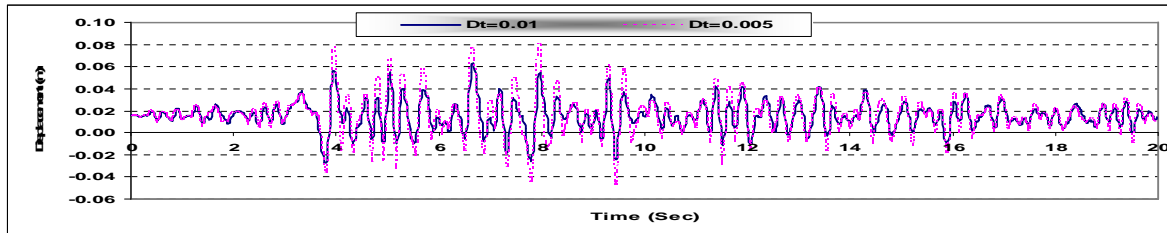


Figure 15 Time history of first principal stress in cracked integration point (First cracking time: 3.2 s) (Case C)

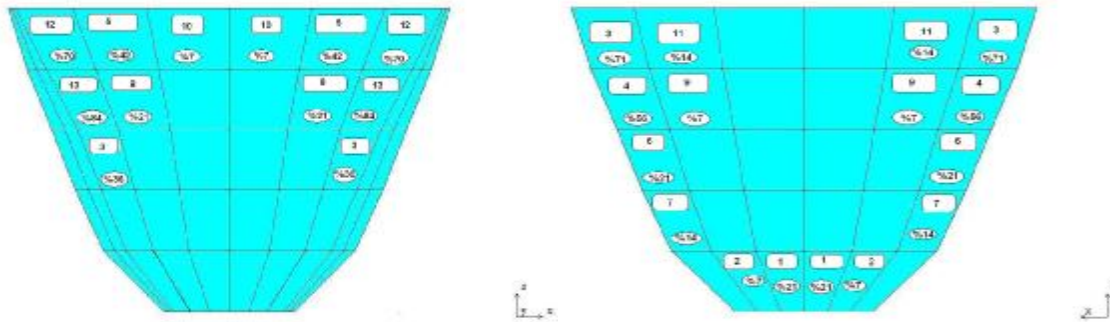


Figure 16 Distribution of damage in dam, Upstream and Downstream (Case C)

5. CONCLUSION

In the present study nonlinear dynamic analysis of arch concrete dam using smeared crack model is presented. A new rotating smeared crack approach is presented. The model consider major characteristic of a reliable crack model. It use energy conservation as localization limiter and for mesh objectivity , the softening could be initiate in each of the principal directions and shear retention factor can calculated and updated based on softening state of element . Another important advantage of the proposed model is that the cracking is allowable on integration point's level and there is not any need to averaging the element quantities on its domain. Thus larger elements could be used for crack analysis.

The hydrodynamic effect of upstream reservoir is considered by accurately. The absorbing boundary conditions, free surface boundary condition and the far field boundary condition was considered properly, also compressibility of fluid was considered. The modified staggered model was proposed to fluid structure interaction modeling. The accuracy and validity of the proposed models and the developed software (GFEAP) were established using the

available numerical results and found that there is an excellent agreement between them. Finally using the developed code based on proposed models, the complete nonlinear dynamic analysis of Morrow Point arch dam was done. Results shown that the proposed crack model has high performances without any instability of model. The use of suitable damping mechanism which affects the crack pattern is emphasized. Small time steps which have high influence on the crack pattern in the dam are also crucial.

REFERENCES

- 1] NRC, (1990), "Earthquake Engineering for Concrete Dams: Design, Performance, and Research needs" National Research Council
- 2] ACI (1998), "Finite Element Analysis of Fracture in concrete structures : State-of-the-Art " American Concrete Institute, ACI 446.3R-97
- 3] Pekau, O.A., Chuhan, Z., Lingmin, F. (1991) "Seismic fracture of concrete gravity dams", *Earthquake Engineering, Structural Dynamics* **Vol.20**, 335-354
- 4] Feng, L.M., Pekau, O.A., (1996) "Cracking analysis of arch dams by 3D boundary element method", *Journal Of Structural Engineering*, **Vol.122**, No.6
- 5] Al-Eidi, B., Hall, J.F. (1989) "Non-linear earthquake response of concrete gravity dam, Part 1 : Modeling", *Earthquake Engineering and Structural dynamics*, **18**, 837-851
- 6] Al-Eidi, B., Hall, J.F. (1989) "Non-linear earthquake response of concrete gravity dam, Part 2 : Behavior", *Earthquake Engineering and Structural dynamics*, **18**, 85-865
- 7] Gunglun, W., Pekau, O.A., Chuhan, Z., Shaumin, W. (2000) "Seismic fracture analysis of concrete gravity dams based on nonlinear fracture mechanics", *Engineering Fracture Mechanics* **65** PP. 67-87
- 8] Battacharjee, S.S., Leger, P., (1992) "Concrete Constitutive model for Non-Linear seismic analysis of gravity dams State-of-the-art", *Canadian Journal of civil engineering*, **19**, 492-509
- 9] Ghrib, F., Tinawi, R. "An application of damage mechanics for seismic analysis of concrete gravity dams", *Earthquake Engineering and Structural Dynamics*, **Vol. 24**, PP.157-173 ()
- 10] Faria, R., Oliver, J., Cervera, M. (1998) "A strain-based plastic viscous damage model for massive concrete structures", *International Journal of Solids Structures*, **Vol.35, No.14**, pp.1533-1558
- 11] Mirzabozorg, G. (2005), "Non-Linear behavior of mass concrete in three-dimensional problems using a smeared crack approach", *Earthquake Engineering and structural dynamics* **34** : 247-269
- 12] Mirzabozorg, G. (2004), "Damage mechanics approach in seismic analysis of concrete gravity dams including dam-reservoir interaction", *European earthquake engineering* **3**
- 13] Moradloo, J. (2007), "Nonlinear dynamic analysis of arch concrete dam considering large displacements" PhD Thesis, Department of Civil engineering, TMU
- 14] Lin, G., Hu, Z., Xiao, S., Li, J. (2004), "Some problems on the seismic design of large concrete dam", *13th World Conference on earthquake engineering*, Vancouver, B.C., Canada, August 1-6